Effect of non-axisymmetric magnetic perturbations on profiles at ASDEX Upgrade

R. Fischer[1], C.J. Fuchs[1], B. Kurzan[1], R.M. McDermott[1], T. Pütterich[1], S.K. Rathgeber[1], W. Suttrop[1], E. Viezzer[1], M. Willensdorfer[2], E. Wolfrum[1], ASDEX Upgrade Team

[1]*Max-Planck-Institut für Plasmaphysik, EURATOM Association, Boltzmannstr. 2, D-85748 Garching, Germany;* [2]*Institut für Angewandte Physik, Technische Universität Wien, Association EURATOM-ÖAW, A-1040 Vienna, Austria*

Non-axisymmetric Magnetic Perturbations (MPs) were successfully applied at ASDEX Upgrade to substantially reduce the plasma energy loss and peak divertor power load that occur concomitant with type-I Edge Localised Modes (ELMs) [1]. Plasmas with mitigated ELMs show similar energy confinement, plasma density and impurity concentration as the unperturbed reference plasmas. ELM mitigation is observed so far only above an edge density threshold. The type-I ELMs are replaced in the mitigated phase by small-scale and high-frequency edge perturbations (*mitigated ELMs*). In this paper we discuss plasma discharges that are conducted so that three separate phases can be distinguished: A phase covering the onset of MPs, a phase where the threshold density is reached and ELM mitigation starts, and a phase where the MPs are switched off. Electron density n_e and temperature T_e profiles are determined with an Integrated Data Analysis approach combining lithium beam (LIB), interferometry and ECE diagnostics [2] and Z_{eff} profiles [3] combining various CXRS diagnostics which also provide ion temperature T_i, radial electric field E_r, and poloidal v_{pol} and toroidal v_{tor} velocity profiles. The profiles are averaged over the time intervals specified, except for the duration of type-I ELM crashes which are removed. The mitigated ELMs are not filtered.

Density profiles as a function of the major radius, $n_e(R)$, at the LIB position ($z = 0.326$ m above the midplane) and relative to the separatrix position, $n_e(R - R_{sep})$, before (black lines) and after (red lines) the onset of MPs are shown in the left panel of Fig. 1 for a pair of plasma discharges (#27029 and #26989) that differ by the orientation of the $n = 2$ MP (Fig. 1, right panel). The ELMs are not mitigated in these time intervals. The edge and scrape-off layer parts of the profile are determined by the LIB data whereas the pedestal-top densities are mainly determined by the edge interferometry channels. The $n_e(R)$ profiles with MPs switched on and off coincide very well with a displacement < 1 mm for both discharges. There is no significant change in the pedestal-top n_e nor in the edge slope. The statistical uncertainties of the profiles are small due to the large averaging time interval. Systematic uncertainties can arise from the edge interferometry channels which are mapped to an equilibrium coordinate system and from

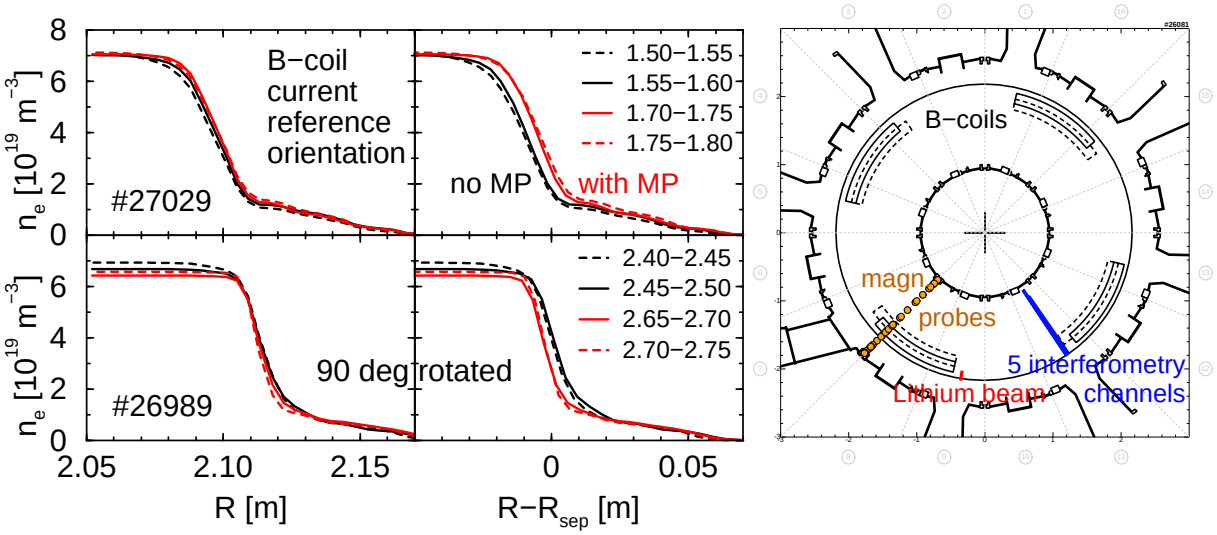

Figure 1: *Left: Density profiles before (black) and after (red) the onset of MPs for two discharges with 90 degree-rotated MP rotation. Right: Toroidal view of ASDEX Upgrade with positions of MP coils, magnetic probes (brown), lithium beam (red) and interferometry (blue).*

the LIB atomic data depending on the temperature profiles. Both systematic uncertainties affect mainly the n_e value and profile shape close to the pedestal top but their effect on profile alignment is small. After mapping to $R - R_{sep}$ the displacement between the profiles before and after the onset of MPs is about 4 mm in opposite directions for the pair of discharges. The profile displacement is an artifact of the CLISTE interpretative code which uses magnetic probe data at a single toroidal location wrongly interpreted by the code as being axisymmetric. For #27029 the reconstructed separatrix position with MPs is about 4 mm at smaller major radius than the true separatrix position. This results in an apparent outward (inward) shift of the profiles for #27029 (#26989). Direction and amplitude of the profile displacement is consistent with field-line tracing calculations [4]. For odd up/down-parity, the radial flux surface deformation is maximum at the midplane between upper and lower MP coils. Therefore, the separatrix shifts at the positions of the LIB (and the magnetic probes) in opposite directions for reference and 90 degree-rotated orientation, respectively. The observation that $n_e(R)$ is not shifting is due to the plasma position control compensating the true separatrix R_{sep} shift (see also [5]).

In contrast to minor changes of the pedestal-top n_e, the pedestal-top T_e is not conclusive. While for #27029 T_e decreases significantly from 420 eV to 360 eV after the onset of the MPs, for #26989 no significant change of T_e is observed.

Figure 2 shows n_e profiles in the second phase shortly before and after the onset of ELM mitigation for #26081 at around 2.8-2.9 s as a function of ρ_{pol} (left panel) and R (right panel). The most prominent change is the density increase at the pedestal top from 5.5×10^{19} m^{-3}

to 6.0×10^{19} m^{-3} within 100-200 ms. There is nearly no change in the gradient between $\rho_{\rm pol} = 0.98 - 1.02$ or $R = 2.08 - 2.11$ m. As here the MPs are on in all cases, the radial profile positions in the two coordinate systems show only minor differences. $n_{\rm e}(R)$ evolves actually only at the pedestal top whereas there are some minor changes in $n_{\rm e}(\rho_{\rm pol})$.

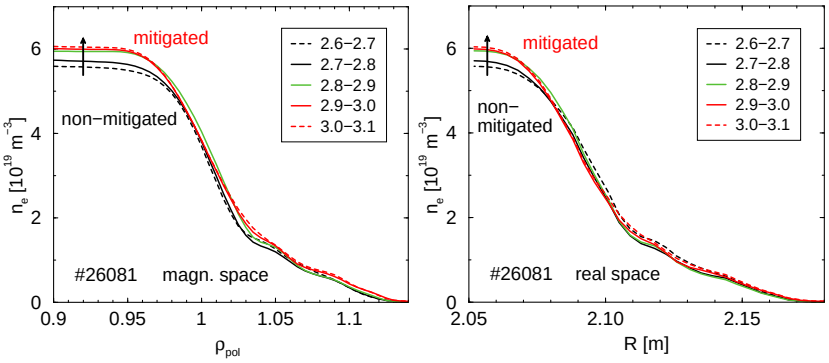

Figure 2: *Density profiles before (black), during (green), and after (red) the transition to the ELM mitigation for two coordinate systems $n_{\rm e}(\rho_{\rm pol})$ (left) and $n_{\rm e}(R)$ (right).*

Figure 3 shows the temporal evolution of $n_{\rm e}$, $T_{\rm e}$, and pressure $p_{\rm e}$ at the pedestal top. No changes are seen in $n_{\rm e}$, $T_{\rm e}$, and $p_{\rm e}$ before or after the onset of the MPs at 2.0 s. Although type-I ELM crashes are removed there is still significant scatter of all three quantities at the pedestal top due to the recovery phase after each large ELM. In the period $t = 2.1 - 2.8$ s $n_{\rm e}$ increases

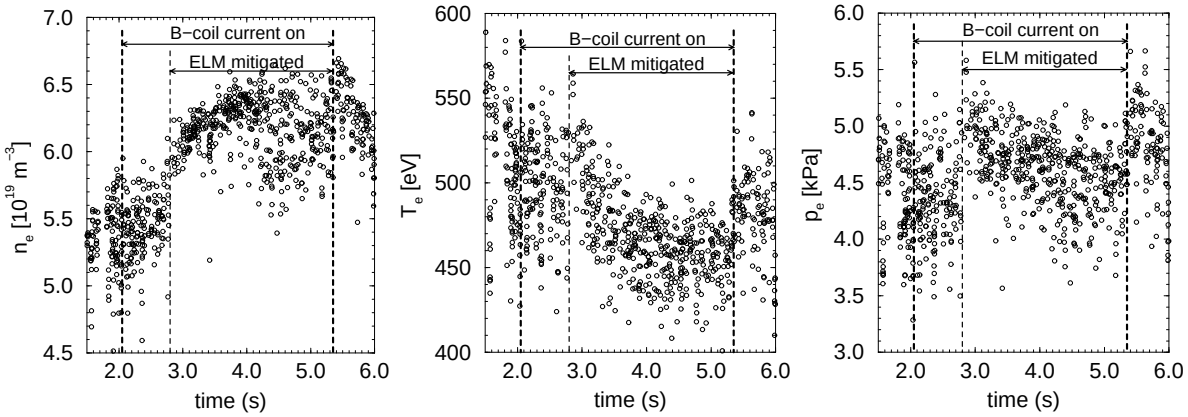

Figure 3: *Pedestal-top electron density, temperature and pressure at $\rho_{\rm pol} = 0.95$ (#26081).*

slightly to about 5.8×10^{19} m^{-3} which can be seen also by an increase of about 8% of the line-averaged $n_{\rm e}$ in the edge interferometry channel. At 2.8 s the ELM mitigated phase starts with a density increase of about 0.4×10^{19} m^{-3} within about 0.2 s. $T_{\rm e}$ and $p_{\rm e}$ increase by about 30 eV and 0.8 kPa, respectively. There is no external trigger such as a change in the density fuelling rate or a change in the heating scenario. After the onset of mitigation of type-I ELMs the scatter of $n_{\rm e}$ at the pedestal top is reduced although small bursts are still present. At about 3.5-4.5 s the scatter increases again and reaches a rather large scattering level until the end of the MP phase at 5.3 s. Similar scattering behaviour is seen also for $T_{\rm e}$ and $p_{\rm e}$ at the pedestal top. In contrast to the increasing pedestal-top $n_{\rm e}$ saturating at about 6.5×10^{19} m^{-3}, $T_{\rm e}$ decreases after the short

increasing phase concomitant with an observed decreasing ion temperature T_i. This results in a pedestal-top p_e which saturates nearly at the same value as just before the ELM mitigated phase. This temporal evolution is observed in a wide variety of plasma discharges.

Figure 4 shows profiles of $n_e(R)$ and $n_e(R-R_{sep})$ in the third phase shortly before and after the MPs are switched off at around 5.3-5.4 s. The apparent shift of the separatrix position is reversed as expected. In contrast to the early phase, the pedestal-top density shows a further transient increase concurrent with a steepening of the gradient.

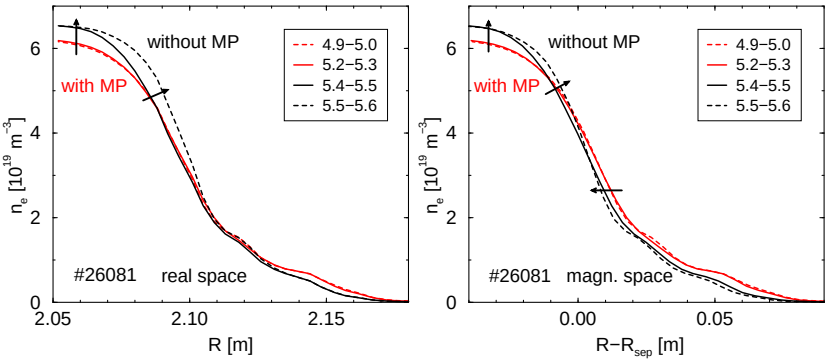

Figure 4: *Density profiles before (red) and after (black) the MPs are switched off for a real (left) and magnetic (right) coordinate system.*

Figure 5 shows the temporal evolution of Z_{eff} averaged over interferometry lines of sight through the core ($\rho_{pol,min} = 0.1$), mid-radius ($\rho_{pol,min} = 0.4$) and the edge ($\rho_{pol,min} = 0.7$). Though the temporal variation in $< Z_{eff} >$ and the relative changes of the various lines of sight are small, three phases can be identified: Constant Z_{eff} before ELM mitigation with and without MPs, decreasing Z_{eff} in the ELM mitigated phase, and a small increase after the MPs are switched off. The statistical uncertainty from the scatter of $< Z_{eff} >$ is small. Although there is a quite large systematic uncertainty of 10-20% mainly due to uncertainties in n_e, no impurity accumulation is observed in the ELM-mitigated phase.

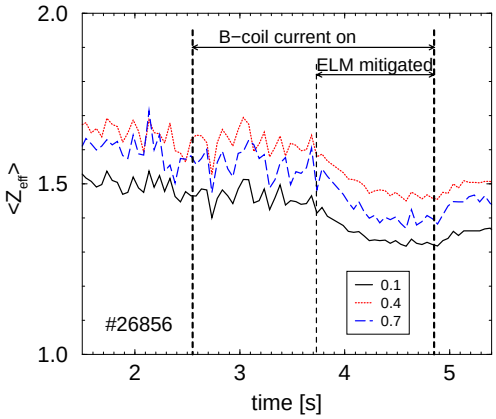

Figure 5: *Temporal evolution of the Z_{eff} profile averaged over core (black), mid-radius (red) and edge (blue) lines of sight.*

Nearly no differences of v_{pol}, v_{tor}, and hence E_r profiles are observed with and without MPs consistent with minor changes in the pressure profile.

References

[1] W. Suttrop et al. *Phys. Rev. Lett.*, 106:225004, 2011, and in *this conference*, I2.109, 2011.
[2] R. Fischer, et al. *Fusion Sci. Technol.*, 58:675–684, 2010.
[3] S.K. Rathgeber, et al. *Plasma Phys. Control. Fusion*, 52:095008, 2010.
[4] J.C. Fuchs et al. In *this conference*, P1.090, 2011.
[5] B. Kurzan et al. In *this conference*, P4.048, 2011.